



**HAL**  
open science

## Mnesic Evocation: An isochron-based analysis

Hedi Ben Amor, Jacques Demongeot, Nicolas Glade

► **To cite this version:**

Hedi Ben Amor, Jacques Demongeot, Nicolas Glade. Mnesic Evocation: An isochron-based analysis. Advanced Information Networking and Applications. The 2010 IEEE International Workshop on Bioinformatics and Life Science Modeling and Computing (BLSMC 10)., Apr 2010, Perth, Australia. pp.745 - 750, 10.1109/WAINA.2010.90 . hal-00511250

**HAL Id: hal-00511250**

**<https://hal.science/hal-00511250>**

Submitted on 24 Aug 2010

**HAL** is a multi-disciplinary open access archive for the deposit and dissemination of scientific research documents, whether they are published or not. The documents may come from teaching and research institutions in France or abroad, or from public or private research centers.

L'archive ouverte pluridisciplinaire **HAL**, est destinée au dépôt et à la diffusion de documents scientifiques de niveau recherche, publiés ou non, émanant des établissements d'enseignement et de recherche français ou étrangers, des laboratoires publics ou privés.

# Mnesic Evocation: An isochron-based analysis

Hedi Ben Amor

Laboratoire TIMC-IMAG

Techniques de l'Ingénierie Médicale et de la Complexité  
Informatique, Mathématiques et Applications de Grenoble

Universit Joseph Fourier CNRS - UMR 5525

Domaine de la Merci, 38700 La Tronche, France

Email: hedi.ben-amor@imag.fr

Telephone.: +33-4-56-52-00-26

Fax: +33-4-76-76-88-44

Jacques Demongeot

Laboratoire TIMC-IMAG

Techniques de l'Ingénierie Médicale et de la Complexité  
Informatique, Mathématiques et Applications de Grenoble

Universit Joseph Fourier CNRS - UMR 5525

Domaine de la Merci, 38700 La Tronche, France

Email: jacques.demongeot@imag.fr

Telephone.: +33-4-56-52-01-08

Fax: +33-4-76-76-88-44

Nicolas Glade

Laboratoire TIMC-IMAG

Techniques de l'Ingénierie Médicale et de la Complexité  
Informatique, Mathématiques et Applications de Grenoble

Universit Joseph Fourier CNRS - UMR 5525

Domaine de la Merci, 38700 La Tronche, France

Email: nicolas.glade@imag.fr

Telephone.: +33-4-56-52-00-26

Fax: +33-4-76-76-88-44

**Abstract**—Mnesic evocation occurs under the action of a stimulus. A successful evocation is observed as the overrun of a certain threshold of the neuronal activity followed by a medical imaging instrument like a PET-scanner. Within the neural system, this successful evocation corresponds to an effective activity that induces other activations in other parts of the brain and conscious actions. Populations of coupled neuronal oscillators can dynamically store information in the form of a periodic attractor of large dimension. In this context, the overrun of such an activity threshold is due to a maximization of the global activity of the population of oscillators. It is allowed by a synchronized activity of the – neuronal – oscillators, which can be provided by the action of an external stimulation. One can hold this process as an elementary process of mnesic evocation. We use an isochron-based analysis to understand the relevant aspects of this synchronization phenomenon. The temporal gap resulting from the perturbation of a large population of uncoupled oscillators (initially distributed in an equal manner on the latent phase) gives us a direct characterization of the phase space. We obtain a method to classify the phase space into fast and slow synchronization regions, thus allowing a qualitative understanding of the behaviour adopted by oscillators in response to perturbations.

## I. INTRODUCTION

By studying the isochrons profil of a dynamical system having a limit cycle attractor, one can classify the phase space into different regions : fast and slow synchronization regions. A population of oscillators having the same dynamics can be synchronized via a common perturbation undergone in a certain direction and having a sufficient amplitude to bring them all to fast or slow synchronization areas.

In this article, we focus on 3 different dynamical systems, the van der Pol oscillator a well-known self-driven dynamical system [1], the phospho-fructo kinase (PFK) that can show

in certain conditions periodic dynamics of the fructose-6-phosphate (the product) and the available chemical energy (ATP/ADP) [2], and more particularly on the Wilson-Cowan neuronal oscillator. The Wilson-Cowan model [3] consists in a couple of inhibitory and excitatory neurons. Its dynamical behaviour exhibits a limit cycle attractor and an unstable equilibrium at the origin.

We highlight the synchronization phenomena and their analysis, starting with a description of the isochron-based analysis and the maximum phase shift analysis. We determin the isochrons of the limit cycles of these systems in their whole phase spaces. Then we perform several simulations (perturbation and relaxation) which show correlations between phase synchronization and the amplitude of perturbation through a measure of the maximum phase shift. Then we discuss about their importance in the understanding of the mnesic evocation process.

### A. Definition of the isochrons

Let us consider the space  $E \subset \mathbb{R}^n$  (where  $\mathbb{R}$  is the set of the real numbers) of all states of a dynamical system and the times set  $T \subset \mathbb{R}$  (containing time 0), and denote by  $x(t)$  the state of the system at time  $t$ . A trajectory (or flow)  $\varphi$  is an application from the Cartesian product  $E \times T$  onto  $E$  defined by:  $\forall (x, t) \in E \times T$ , then: (i)  $\varphi(x, t) = x(t)$ , (ii)  $x(0) = x$ , (iii)  $\varphi(\varphi(x, t), s) = \varphi(x, t + s)$ . The orbit of a state  $y$  iterated by the flow  $\varphi$  is the set of points  $O(y) = \{\varphi^j(y)\}_{j \in T}$ .

We define the Birkhoff limit set  $L(x)$  of any state  $x$  of  $E$  taken as initial condition of the trajectory  $\varphi(x, \cdot)$ , as the set of temporal accumulation points of this trajectory. If  $B(y, \varepsilon)$  denotes the set of states at distance of  $y$  less than  $\varepsilon$  ( $B(y, \varepsilon)$

is reduced to  $\{y\}$  in the discrete case):  $L(x) = \{y \in E; \forall \varepsilon > 0, \forall t \in T, \exists s \in T / s > t \text{ and } O(\varphi(x, s)) \cap B(y, \varepsilon) \neq \emptyset\}$

The attractor basin  $B(A)$  of a subset  $A$  of  $E$  is the set of all initial conditions  $x$  not in  $A$ , but such as  $L(x) \subset A$ . Let us denote  $L(A) = \cup_{x \in A} L(x)$ .  $\bar{A}$  is the set  $A$  completed by all possible shadow trajectories [4]. An attractor  $A$  verifies [5], [6]:

- i)  $A$  is a fixed set for the composed set operator  $LoB : A = L(B(A))$ , where
- ii) there is no set  $C$  such as  $A \subset C \subset \bar{A}, C \neq A$ , verifying i),
- iii) there is no set  $D \subset A, D \neq A$ , verifying i) and ii).

An attractor  $A$  is invariant in the dual operations consisting firstly in considering all the trajectories of its basin from all initial conditions not in  $A$ , but finishing their life in  $A$ , and secondly to restrict them to their ends of life (Figure 1).

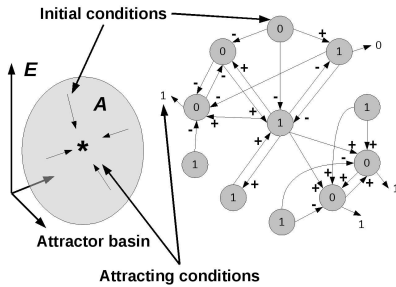


Fig. 1. Definition of an attractor (the character 'star') and its basin (the gray bubble) in the case of a Boolean network, whose the states space  $E$  is the hypercube  $\{0, 1\}^{11}$  (left). Initial conditions are indicated in the gray disks and attracting conditions for the majority rule and synchronous iterations (the state of a node equals 1 if its activating neighbours in state 1 are equally or more numerous than the inhibiting ones) are given outside blue disks (right).

Let us suppose now that the attractor  $A$  is a limit cycle, *i.e.*, if we denote by  $p$  the period of the limit cycle,  $A = \{a_0, a_1 = \varphi(a_0, 1), \dots, a_{p-1} = \varphi(a_0, p-1)\}$  and there is a natural isomorphism  $\psi$  between  $A$  and the set  $S = \{0, \dots, \tau-1\}$ . By denoting  $T_s = \{t \in T / t = s + k\tau\}_{k \in \mathbb{N}, s \in S}$  we have:  $T = \cup_{s \in S} T_s$ .

The isochron  $I_s$  of phase  $s$  is the attractor basin of  $\{\psi(s) = a_s\}$  for the flow  $\varphi_s$  (equal to  $\varphi$  on  $E \times T_s$ ) and  $B(A) = \cup_{s \in S} I_s$ . If  $T = \mathbb{R}^+$  (the positive real numbers set),  $I_s$  is transversal to  $A$ , *i.e.*, the tangent vector to  $I_s$  at the state  $a_s$  is not tangent to  $A$  [7], [8].

Examples of isochrons of some dynamical systems are shown below in Figure 2. The fibration of equally phase-distributed isochrons is a good tool for analysing the phase space. The convergence (resp. the divergence) of isochrons indicates a slow synchronization region (resp. a fast synchronization region). This furnishes a quantitative information about the direction and the strength of the perturbation to perform in order to synchronize a homogeneous population of oscillators.

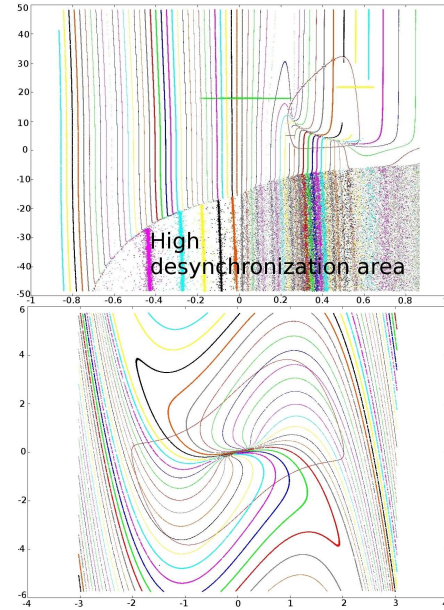


Fig. 2. **Examples of Isochrons of 2 dynamical systems.** (Up) A non-symmetrical system: the PFK enzymatic balance. Isochrons and the limit cycle attractor of the PFK system obtained for a very high precision ( $> 10^6$ ). Note that the region in the bottom is very sensitive to numerical imprecision. In this region, the isochrons are overlapped. This indicates a sensitivity to numerical precision and corresponds to a slow synchronization region. (Down) Isochrons and the limit cycle attractor of the van der Pol oscillator. Fast (resp. slow) synchronization regions, or isochron divergence (resp. isochron convergence) regions of equally phase-distributed isochrons, are located overhead and underneath (resp. on the right and on the left) of the limit cycle in the phase space.

### B. Numerical resolution of isochrons

All points delayed by a period  $T$  (period of the limit cycle) are on the same isochron because they have the same latent phase. The determination of these points can be done by using numerical methods. Whatever the numerical method used is, checking if points of the state space belong to the isochron of a chosen phase can be obtained by verifying, when they converge until the attractor via the equations of the dynamical system, if they admit that phase of the attractor once considered a certain limit. Several numerical methods are possible: a systematic exploration of the state space by dividing it in small areas, a random exploration in all the state space, or a local random exploration with a guidance of the research area along a direction given by the points already founded (a kind of intelligent paintbrush). We pull out a point of the state space randomly, then we compute a discrete version of the differential equations until the trajectory reaches for the first time a point belonging to a neighbourhood of fixed thickness  $10^{-k}$  of the attractor, where  $k$  is a thickness parameter. The phase of this point on the attractor is memorized. This phase minus the phase of the nearest isochron of interest is compared to a tolerance value in order to determine whether this point can be considered as belonging on the isochron or not. This tolerance value is equal to  $\frac{T}{2np}$  (Figure 3) where  $T$  is the period of the attractor considered as a limit cycle,  $n$  is the number of isochrons considered and  $p \in [1, +\text{inf}[$  is a precision

parameter.

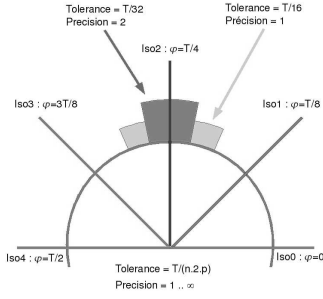


Fig. 3. **Graphical description of the measure of precision** Let us consider 8 isochrons equally spaced. The largest acceptable tolerance is  $T/16$ , i.e. the phase interval between 2 isochrons is equally divided. The precision parameter is used to express the tolerance parameter as follow:  $Tolerance = T / (Precision * 2 * N_{isochrons})$

### C. Maximum phase shift computation

Once considered a population of uncoupled oscillators of same nature, it may be of interest to have a measure of the synchronization that occurs after a perturbation translating the state of all the oscillators to an other region at the same time, *i.e.* conserving that way the shape of the limit cycle (see Figures 8 and 9). The isochronal fibration gives a qualitative idea of the phase shift or on the contrary of the resynchronization which may result from a perturbation affecting this population. The divergence (resp. convergence) of equally distributed isochrons in a particular region of the phase space means indeed that this region is a fast (resp. slow) synchronization one. A quantitative measurement can be calculated from this fibration. We computed the phase shift between the two isochrons containing the set of  $n$  points  $(P_i)_{i \in [1, n]}$  obtained after a translation of the limit cycle as follows:

- The phase  $\phi_i$  of each  $P_i$  is calculated as described in the previous section.
- The vector  $[P_i]_i$  is sorted by order of the increasing values of  $\phi_i$ .
- The vector  $((\Delta\Phi_{i,i+1})_{i \in [1, n-1]}, \Delta\Phi_{n,0})$  is determined.  $\Delta\Phi_{i,i+1} = \phi_{i+1} - \phi_i$  for  $i \in [1, n-1]$  and  $\Delta\Phi_{n,0} = 2\pi - (\phi_n - \phi_0)$ .
- The maximum phase shift is  $\Delta\Phi_{Max} = 2\pi - Max((\Delta\Phi_{i,i+1})_{i \in [1, n-1]}, \Delta\Phi_{n,0})$ .

Those steps are repeated for several values of the amplitude between 0 and  $R_{max}$  (maximum perturbation). When the system is symmetrical, we compute the maximum phase shift along an arbitrary direction of perturbation 10. This is not valid when the dynamical system is asymmetrical like the phospho-fructo kinase (PFK) system (see Figure 4).

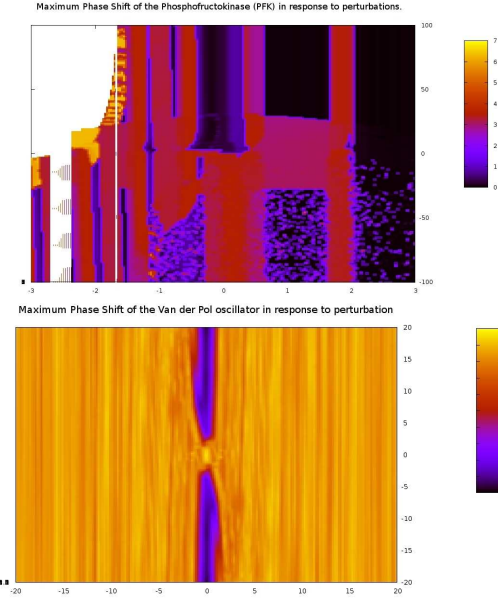


Fig. 4. **Maximum phase shift of the PFK (Up) and the van der Pol (Down) oscillators in response to perturbations** (Up) The maximum phase shift of the PFK. (Down) The maximum phase shift of the van Der Pol. Dark (resp. bright) colors correspond to fast (resp. slow) synchronization regions. White regions correspond to regions where the phase is not well-defined (very strong sensitivity to numerical imprecision). This synchronization map is very irregular and clearly shows that it is hard to synchronize the PFK (Up) due to a (strong non linearity and asymmetry of the system). Synchronizing the whole system needs to choose very precisely the direction and amplitude of the perturbations. This is very different for the van der Pol (Down) system where regions of synchronization (underneath and overhead) and desynchronization (on the right and on the left) are well defined and localized in the phase space.

## II. MNESIC EVOCATION

Let us consider a network (neural or genetic) made of several subsystems, like modules, identical or different, and weakly or strongly connected: in Figure 5, M1 is an arbitrary subnetwork and M2 is made of a simplified Hippocampus one-layered network, with one Cyto-Architectural 1 (CA1) and one Cyto-Architectural 3 (CA3) pyramidal neuron, one Entorhino-Cortical neuron (EC) and one Inter-Neuron (IN), all interconnected. If we simplify this module in a subnetwork of size 2, we obtain a structure called negative regulon, with one negative circuit and 2 positive self-loops. We will consider in the following that this subnetwork is sequentially repeated in a chain of modules, each of them being weakly linked to the following at the level of the CA3 neurons (the  $X_i$ 's in Figure 6): CA3 neurons send axons with excitatory synapses to CA1 and CA3 neurons, these latter sending axons with excitatory synapses to EC neurons through the Subiculum (SB), and EC forming global inhibitory connections with CA3 neurons through Inter-Neurons (IN) of Dentate Gyrus (DG) [9], [10], [11], [12], [13].

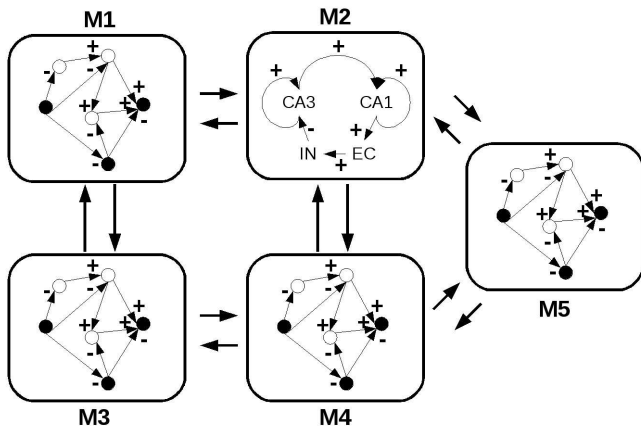


Fig. 5. Modular structure, in which the module M1 is arbitrary and M2 represents Hippocampus subnetwork.

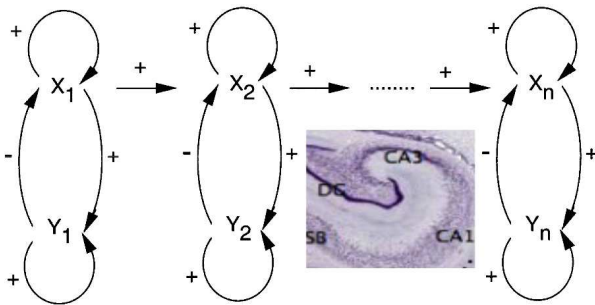


Fig. 6. Scheme of a sequential modular structure made of a chain of negative regulons, where X1 represents the activity of CA3 and X2 the activity of CA1 (see anatomy of CA3, CA1, DG and SB in the cartouche)

The Wilson-Cowan system WC [3] used to simulate the dynamics of a subnetwork represented by a negative regulon (Figure 6) is given by  $2n$  differential equations:  $\forall i = 1, \dots, n$ ,  $dX_i/dt = -X_i/a + \tanh(bX_i) - \tanh(bY_i) + kX_{i-1}$ ,  $dY_i/dt = -Y_i/a + \tanh(bX_i) + \tanh(bY_i)$ . This system is closed to a Hopfield neural network, when  $b$  is positive and large, and  $a$  is negative and large [14]. Trajectories and isochrons of WC are represented in Figure 7, showing fast (resp. slow) regions, *i.e.*, zones where the flow runs fast (resp. slow).

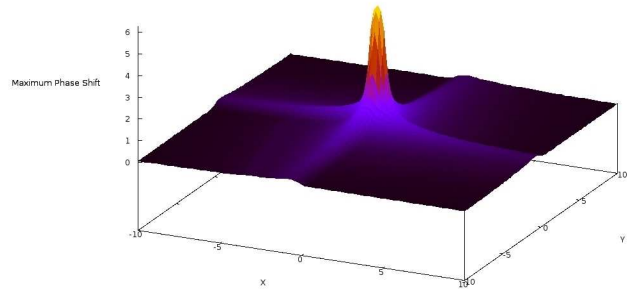
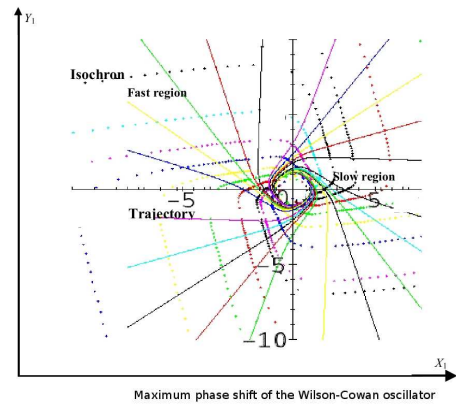


Fig. 7. (Up) Isochronal and trajectory landscape for the Wilson-Cowan dynamics of a negative regulon, showing fast (resp. slow) regions, where the velocity is high (resp. low). (Down) Fast (resp. Slow) synchronization regions in dark colors (resp. bright colors) of the Wilson-Cowan oscillator obtained by computing the maximum phase shift in response to perturbations.

When the system WC is stimulated through a perturbation  $S$  translating all the initial conditions on the limit cycle  $C$  into a fast region (Figure 8 and 9), then all the return trajectories go to the same phase  $x_1$ , provoking a synchronization of all the activities  $X_i$ 's. In other terms, if the  $X_i$ 's before the stimulation are dispatched uniformly on the limit cycle  $C$ , then their sum denoted  $A(t) = \sum_{i=1, \dots, n} X_i(t)$  is about zero, because the positive values of the  $X_i$ 's are compensated by the negative ones. If the  $X_i$ 's run in phase,  $A(t)$  behaves like  $nX_i(t)$  and can be detected for example by a Pet-scanner of a functional MRI device (Figure 11). Some dynamical systems like the PFK system are not symmetrical and have numerous regions of slow synchronization as revealed by their isochron fibration (fig. 2) and by their synchronization map (fig. 4). In those cases, translating the system to these regions causes a loss of the synchrony of the  $X_i$ 's.

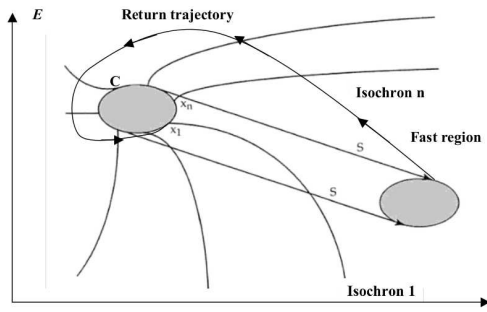


Fig. 8. Synchronizing stimulation  $S$  translating the limit cycle  $C$  in a fast region of the states space  $E$

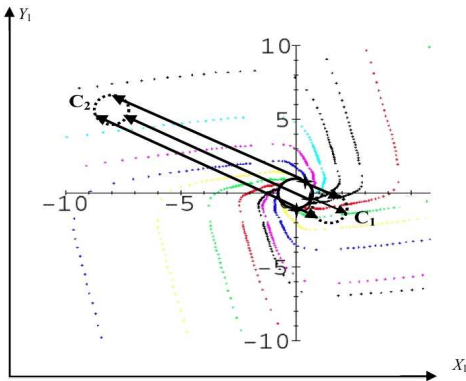


Fig. 9. Isochronal and trajectory landscape with perturbations translating the limit cycle  $C$  either in a desynchronizing slow region ( $C_1$ ), or in a synchronizing fast region ( $C_2$ )

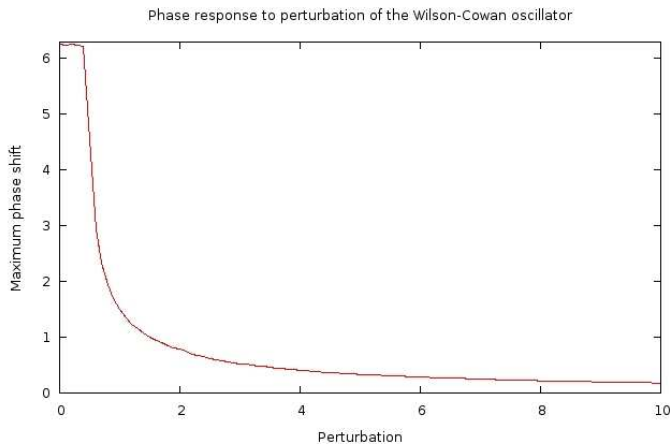


Fig. 10. The phase shift between the two isochrons containing the limit cycle after translating with respect to amplitude of perturbation. Slow (resp. fast) synchronization area are situated (qualitatively) for an amplitude below (resp. above) 2.

If the coupling between the WC subnetworks is made at the level of the CA3 neurons (whose activities are the  $X_i$ 's) is weak (which correspond to a permanent translation to slow synchronization areas 10), then a desynchronization

occurs (Figure 11-1), allowing the exit out the perseveration behaviour (Figure 11-2). If the neuronal activity is noised, the desynchronization obtained with a weak coupling is not perfect (Figure 11-3), as well as the perseveration (Figure 11-4), both behaviours exhibiting a small residual synchronized activity.

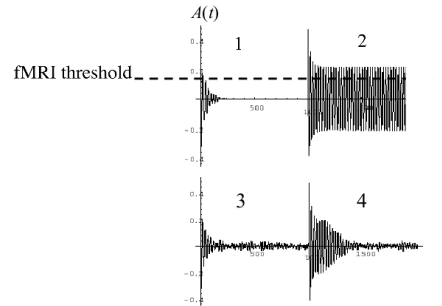


Fig. 11. Post-stimulation global activity  $A(t)$  of CA3 neurons ( $A(t) = \sum_{i=1, \dots, n} X_i(t)$ ), with a weak deterministic intra-CA3 coupling showing a fast desynchronization (1), without coupling showing a perseveration (2), with a weak noised coupling showing a fast desynchronization followed by a residual synchronization (3) and with noise without coupling showing a slow desynchronization (4)

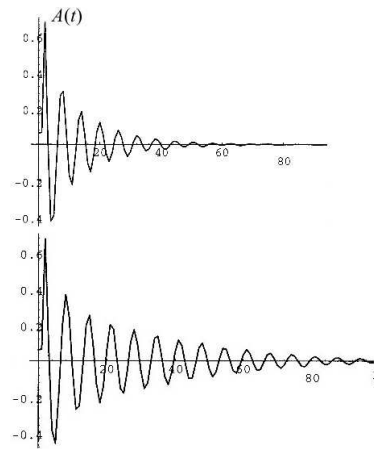


Fig. 12. Post-stimulation global activity  $A(t)$  of CA3 neurons ( $A(t) = \sum_{i=1}^n X_i(t)$ ), with a weak deterministic intra-CA3 coupling showing a fast desynchronization (left), and with a high deterministic intra-CA3 coupling showing a slow desynchronization (right)

In case of synchronization, the global activity  $A(t)$  of the CA3 neurons "evokes" the common limit cycle attractor [15] of the  $X_i$ 's and can be considered as the phenomenologic result of the recall of a mnemonic temporal pattern stored in the network [16], [17]. If the succession of states to be transiently evoked is only a part of this attractor, then a fast desynchronization is needed, which is ensured by a weak coupling (Figure 12). The richness of the stored souvenirs comes from the number and the complexity of the common attractors of the  $X_i$ 's. If their number increases (*e.g.*, from 1 to 2) as well their complexity (*e.g.*, passing from the circular limit cycle coming from a fixed configuration of focus type through a Hopf bifurcation, to

a chaotic behaviour through doubling period bifurcations), then we can locally store and evoke complicated temporal patterns coding for complex cognitive entities or serving for moving objects detection in a complex scene [18]. Such a bifurcations landscape can be simply obtained from the simulation of a fully connected Hopfield network of size 16, involved in a learning process, as shown on Figure 13 [19].

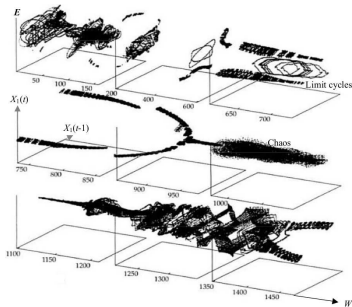


Fig. 13. Bifurcations of the attractors of the dynamics  $(X_1(t-1), X_1(t))$  for the first of 16 neurons fully connected in a classical Hopfield neural network, when a function  $W$  of its synaptic weights  $w_{ij}$  vary during a learning process, showing alternance of chaotic and periodic behaviours

### III. CONCLUSION

The places where the isochrons diverge (resp. converge) are fast (resp. slow) synchronization regions. This allows us to classify the phase space so as to determine the minimal or the suitable strength and direction of perturbation to have an acceptable phase synchronization. Synchronization corresponds to an increase of the global activity of a population of coupled oscillators. The resulting signal in a neural cortex becomes measurable by fMRI. Such a synchronized signal reveals the occurrence of a conscious event like mnemonic evocation. The desynchronization of neurons is then ensured by a weak coupling between oscillators, which in other terms corresponds to a permanent perturbation towards slow synchronization regions. Then, the understanding of the phase synchronization by analysing the phase space constitutes a powerful tool for designing new storage systems based on populations of coupled oscillators, as proposed in [20], and an advance in the researches on the memory and mnemonic evocation.

### ACKNOWLEDGMENT

This work was supported by the Virtual Physiological Human Network of Excellence of the European Community (VPH-NoE).

### REFERENCES

- [1] B. V. der Pol and J. van der Mark, "Frequency demultiplication," *Nature*, vol. 120, pp. 363–364, 1927.
- [2] J. C. D. Ricci, "Influence of phosphoenolpyruvate on the dynamic behavior of phosphofructokinase of *Escherichia coli*," *J. Theor. Biol.*, pp. 145–150, 1995.
- [3] H. R. Wilson and J. D. Cowan, "Excitatory and inhibitory interactions in localized populations of model neurons," *Biophys. J.*, vol. 12, pp. 1–24, 1974.

- [4] R. Bowen, "Limit sets for axiom A diffeomorphisms," *J. Differential Equations*, vol. 18, pp. 333–339, 1975.
- [5] M. Cosnard and J. Demongeot, "On the definitions of attractors," *Lecture Notes in Mathematics*, vol. 1163, pp. 23–31, 1985.
- [6] —, "Attracteurs: une approche déterministe," *C. R. Acad. Sc. Maths. Série I*, vol. 300, pp. 551–556, 1985.
- [7] J. Guckenheimer, "Isochrons and phaseless sets," *J. Math. Biol.*, vol. 1, pp. 259–273, 1975.
- [8] E. Freire, A. Gasull, and A. Guillamon, "Limit cycles and Lie symmetries," *Bull. Sci. Maths*, vol. 131, pp. 501–517, 2007.
- [9] G. Buzsáki, "Feed-forward inhibition in the hippocampal formation," *Prog. Neurobiol.*, vol. 22, pp. 131–153, 1984.
- [10] M. A. Gluck, "Computational models of hippocampal function in memory," *Hippocampus*, vol. 6, pp. 565–566, 1996.
- [11] S. Hefft and P. Jonas, "Asynchronous GABA release generates long-lasting inhibition at a hippocampal interneuron-principal neuron synapse," *Nature Neuroscience*, vol. 8, pp. 1319–1328, 2005.
- [12] R. Bartesaghi, M. Migliore, and T. Gessi, "Input-output relations in the entorhinal cortex-dentate-hippocampal system: evidence for a non-linear transfer of signal," *Neuroscience*, vol. 142, pp. 247–265, 2006.
- [13] M. Mori, B. H. Gähwiler, and U. Gerber, "Recruitment of an inhibitory hippocampal network after bursting in a single granule cell," *Proc. Nat. Acad. Sci. USA*, vol. 104, pp. 7640–7645, 2007.
- [14] A. Tonnelier, S. Meignen, H. Bosch, and J. Demongeot, "Synchronization and desynchronization of neural oscillators: comparison of two models," *Neural Networks*, vol. 12, pp. 1213–1228, 1999.
- [15] J. Csicsvari, H. Hirase, A. Czurko, A. Mamiya, and G. Buzsáki, "Fast network oscillations in the hippocampal CA1 region of the behaving rat," *The Journal of Neuroscience*, *RC20*, vol. 19, pp. 1–4, 1999.
- [16] J. Demongeot, M. Kaufman, and R. Thomas, "Positive feedback circuits and memory," *C.R. Acad. Sc. Sciences de la Vie*, vol. 323, pp. 69–79, 2000.
- [17] A. V. Samsonovich and G. A. Ascoli, "A simple neural network model of the hippocampus suggesting its pathfinding role in episodic memory retrieval," *Learn. Mem.*, vol. 12, pp. 193–208, 2005.
- [18] H. Hayashi, K. Nakada, and T. Morie, "Moving object detection algorithm inspired by the sequence detection in the hippocampus and its digital LSI implementation," *International Congress Series*, vol. 1301, pp. 35–38, 2007.
- [19] O. Nérot, "Mémoire par forçage neuronal des dynamiques chaotiques dans les modèles connexionnistes récurrents," Ph.D. dissertation, Université Joseph Fourier, Grenoble, 1996.
- [20] H. Ben-Amor, N. Glade, C. Lobos, and J. Demongeot, "The isochronal fibration: Characterization and implication in biology," *Acta Biotheoretica*, 2010, submitted.